

Phonon Inverse Faraday effect from electron-phonon coupling

Natalia Shabala^{1,*} and R. Matthias Geilhufe^{1,†}

¹*Department of Physics, Chalmers University of Technology, 412 96 Göteborg, Sweden*

(Dated: May 16, 2024)

The phonon inverse Faraday effect describes the emergence of a DC magnetization due to circularly polarized phonons. In this work we present a microscopic formalism for the phonon inverse Faraday effect. The formalism is based on time-dependent second order perturbation theory and electron phonon coupling. While our final equation is general and material independent, we provide estimates for the effective magnetic field expected for the ferroelectric soft mode in the oxide perovskite SrTiO₃. Our estimates are consistent with recent experiments showing a huge magnetization after a coherent excitation of circularly polarized phonons with THz laser light. Hence, the theoretical approach presented here is promising for shedding light into the microscopic mechanism of angular momentum transfer between ionic and electronic angular momentum, which is expected to play a central role in the phononic manipulation of magnetism.

I. INTRODUCTION

Circularly polarized phonons or axial phonons are lattice vibrations with a non-zero angular momentum. These lattice vibrations can induce a magnetization in the material. This magnetization is an example of dynamical multiferroicity, the phenomenon in which the motion of ions in a crystal causes its polarization to vary in time, thus inducing a net magnetization [1–4].

While the gyromagnetic ratio of the phonon hints towards a magnetization in the order of the nuclear magneton, recent experiments using phonon Zeeman effect and magneto-optical Kerr effect [5–10] show that the size of the magnetization resulting from circularly polarized moment is quite significant, with magnetic moments on the order of magnitude of 0.1 – 10 μ_B . This is a promising route for using phonons for magnetic manipulation [11], as has recently been shown on the example of the magnetic switching due to the ultrafast Barnett effect [12]. Here, the Barnett effect [13] describes the magnetization of a nominally nonmagnetic sample due to mechanical rotation, and is the inverse of the so-called Einstein-de-Haas effect [14]. Recently, both effects have been brought into the characteristic time and length-scales of material excitations, and phenomenologically describe the angular momentum transfer between magnetization and phonons [12, 15, 16].

These findings call for a microscopic theory of angular momentum transfer between phonons and electrons for describing the phonon-induced magnetic moments. As a result, multiple microscopic theories of this have been proposed, explaining the size of the phonon-induced magnetic moment, e.g., by inertial effects [17, 18], orbit-lattice coupling [19], spin-orbit coupling [20], orbital magnetization [21], electron-nuclear quantum geometry [22], non-Maxwellian fields [23, 24]. While these approaches show similarities and overlap in

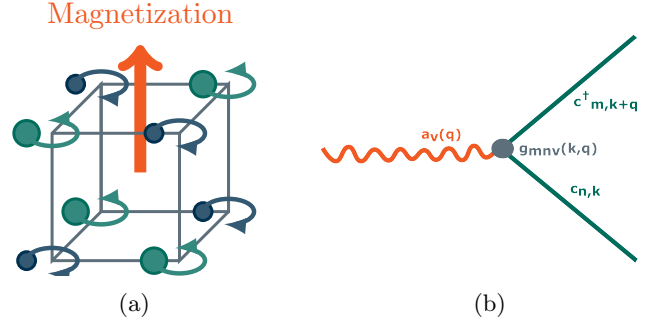


FIG. 1: a) Schematically depicted phonon inverse Faraday effect. b) Vortex diagram of electron-phonon interaction: electron in a state $|n, \mathbf{k}\rangle$ absorbs a phonon of mode ν with a wave vector \mathbf{q} and scatters to a state $|m, \mathbf{k} + \mathbf{q}\rangle$

their formalism, the consensus on the microscopic theory behind the effect has not yet been reached.

In contrast, the optical analogue, i.e., the transfer of spin angular momentum from circularly polarized light to electron spin is well-described by the inverse Faraday effect [25]. Here, the electric field of the light couples to the electron via the dipole-interaction. From a symmetry perspective, the concept of inverse Faraday effect is universal and can be generalized to any circularly polarized vector field, beyond a laser field. Examples comprise axial magnetoelectric effect [26] and the *phonon inverse Faraday effect* [11]. Here, we provide the microscopic theory for the phonon inverse Faraday effect by coupling circularly polarized phonons to electrons via the electron-phonon interaction.

II. PHONON INVERSE FARADAY EFFECT - PHENOMENOLOGICAL THEORY

We start with a phenomenological description of the phonon inverse Faraday effect, similar to Pershan *et al.*

* natalia.shabala@chalmers.se

† matthias.geilhufe@chalmers.se

[25] and the optical inverse Faraday effect. For simplicity, we consider 2-fold degenerate phonon level, with two modes u_μ and u_ν . We are free to introduce a basis transform, e.g., to the circularly polarized basis,

$$\mathbf{u}(t) = \left(\frac{1}{\sqrt{2}}u_R(\hat{\mathbf{e}}_\mu + i\hat{\mathbf{e}}_\nu) + \frac{1}{\sqrt{2}}u_L(\hat{\mathbf{e}}_\mu - i\hat{\mathbf{e}}_\nu) \right) e^{i\omega t}, \quad (1)$$

with $u_R = (u_\mu - iu_\nu)/\sqrt{2}$ and $u_L = (u_\mu + iu_\nu)/\sqrt{2}$. We need define free energy function in terms of phonon mode amplitudes. To fulfill the symmetry criteria of a non-magnetic and inversion symmetric crystal, the thermodynamic free energy has to be invariant under time reversal and space inversion. This gives rise to the following phenomenological coupling between circularly polarized phonons and the magnetic field \mathbf{H} ,

$$F_u = \chi H_z (u_R u_R^* - u_L u_L^*) = i\chi H_z (u_\mu u_\nu^* - u_\nu u_\mu^*). \quad (2)$$

As a result, the magnetization is given by

$$M_z = -\frac{\partial F_u}{\partial H_z} = \chi (u_L u_L^* - u_R u_R^*). \quad (3)$$

From the equation above it becomes evident that an imbalance of circularly polarized phonons induce the DC magnetization of the material. Such an imbalance can be induced by coherent excitation with circularly polarized laser light [5, 6, 12]. However, the effect itself is purely phononic and does not require light. To offer a full picture, we give the phononic Faraday rotation,

$$\Delta\epsilon_R^u = -4\pi \frac{\partial^2 F_u}{\partial u_R \partial u_R^*} = -4\pi\chi H_z, \quad (4)$$

$$\Delta\epsilon_L^u = -4\pi \frac{\partial^2 F_u}{\partial u_L \partial u_L^*} = 4\pi\chi H_z. \quad (5)$$

Hence, in the presence of an applied magnetic field, phonons develop circular polarization.

III. PHONON INVERSE FARADAY EFFECT - MICROSCOPICAL THEORY

In the following we develop the microscopic theory of the phonon inverse Faraday effect. A phonon is the collective excitation of the lattice, i.e., time-dependent displacements of the ions around their equilibrium positions. Hence, phonons introduce a time-dependent perturbation $V(t)$ into the system, $\hat{H} = \hat{H}_0 + V(t)$. We assume that the atom displacements $u_{pj\alpha}$ are sufficiently small and the potential function can be written as a first-order Taylor expansion. Then the perturbation $V(t)$ is given by

$$V(t) = \sum_{pj\alpha} \frac{\partial U}{\partial u_{pj\alpha}} u_{pj\alpha}, \quad (6)$$

where we consider the variation of the potential due to displacement of atom j in Cartesian direction α in a unit cell p .

Before presenting the main result, we outline our approach for a single ion with displacement $\mathbf{u}(t)$. To allow for circular polarization, $\mathbf{u}(t)$ is generally complex. In this case the real-valued perturbation becomes $V(t) = 2\Re[\mathbf{u}(t) \cdot \nabla_{\mathbf{u}} U]$. Hence, we express the time-dependent perturbation as follows,

$$V(t) = v e^{i\omega t} + v^* e^{-i\omega t}, \quad (7)$$

where ω denotes the phonon frequency. Equation (7) gives rise to an effective Hamiltonian in second order perturbation theory [25],

$$\langle a | H_{\text{eff}}(t) | b \rangle = - \sum_n \left[\frac{\langle a | v | n \rangle \langle n | v^* | b \rangle}{E_{nb} - \hbar\omega} - \frac{\langle a | v^* | n \rangle \langle n | v | b \rangle}{E_{nb} + \hbar\omega} \right]. \quad (8)$$

Here, $|n\rangle$ are eigenstates of the unperturbed Hamiltonian, and $E_{nb} = E_n - E_b$ denotes the energy difference between states $|n\rangle$ and $|b\rangle$. We evaluate the effective Hamiltonian (8) and only keep terms giving a contribution to the magnetization as discussed in (3). This allows us to formulate the following revised effective Hamiltonian,

$$\mathcal{H}_{\text{eff}}^{ab}(\mathbf{k}) = -\hbar\omega(\mathbf{u} \times \mathbf{u}^*)_z \times \sum_n \frac{(\langle a | \nabla U | n \rangle \times \langle n | \nabla U | b \rangle)_z}{E_{knb}^2 - \hbar^2\omega^2}. \quad (9)$$

Equation (9) represents a semi-classical solution where the ionic displacement is not quantized. We generalize the single ion case for the entire crystal by introducing a quantized version of the displacement for phonon modes μ and ν :

$$\begin{aligned} u_{p\mu} &= i \sum_{\mathbf{q}} e^{i\mathbf{q} \cdot \mathbf{R}_p} l_{q\mu} (\hat{a}_{q\mu} + \hat{a}_{-q\mu}^\dagger), \\ u_{p\nu} &= \sum_{\mathbf{q}} e^{i\mathbf{q} \cdot \mathbf{R}_p} l_{q\nu} (\hat{a}_{q\nu} + \hat{a}_{-q\nu}^\dagger). \end{aligned} \quad (10)$$

Here, $l_{q\nu} = \sqrt{\frac{\hbar}{2M_0\omega_{q\nu}}}$ is the zero displacement amplitude and M_0 is a reference mass. Operators $\hat{a}_{q\nu}^\dagger$ and $\hat{a}_{q\nu}$ are bosonic creation and annihilation operators. Together the phonon modes (10) form a circularly polarized phonon mode according to equation (1).

To describe the electron-phonon coupling we introduce electron-phonon matrix elements $g_{m\nu}(\mathbf{k}, \mathbf{q})$ which describe the probability amplitude of an electron absorbing a phonon of mode ν and wave vector \mathbf{q} and scattering from state $|n, \mathbf{k}\rangle$ to state $|m, \mathbf{k} + \mathbf{q}\rangle$ [27, 28]. A schematic diagram is given in Figure 1(a). Following Ref. [28], the electron-phonon matrix elements are given by

$$g_{m\nu}(\mathbf{k}, \mathbf{q}) = \langle m, \mathbf{k} + \mathbf{q} | \sum_p l_{q\nu} e^{i\mathbf{q} \cdot \mathbf{R}_p} \frac{\partial U}{\partial u_{p\nu}} | n, \mathbf{k} \rangle. \quad (11)$$

Using equation (10) and equation (11), we extend the single ion effective Hamiltonian (9) and obtain the following effective Hamiltonian for the entire crystal,

$$\mathcal{H}_{\text{eff}}^{ab}(\mathbf{k}) = -i\hbar\omega \sum_{\mathbf{q}} \left[(\hat{a}_{\mathbf{q},\mu} + \hat{a}_{-\mathbf{q},\mu}^\dagger)(\hat{a}_{-\mathbf{q},\nu}^\dagger + \hat{a}_{\mathbf{q},\nu}) \right. \\ \left. \times \sum_n \frac{g_{an\mu}(\mathbf{k}, \mathbf{q})g_{bn\nu}^*(\mathbf{k}, \mathbf{q}) - g_{an\nu}(\mathbf{k}, \mathbf{q})g_{bn\mu}^*(\mathbf{k}, \mathbf{q})}{E_{knb}^2 - \hbar^2\omega^2} \right]. \quad (12)$$

We note that equation (12) makes no assumptions on the material and represents the main theoretical result of our paper.

Relating to the recent finding of the large dynamical multiferroicity in SrTiO₃ [5] we discuss the effective Hamiltonian (12) for cubic symmetry and an infrared active optical phonon mode with T_{1u} symmetry. The electronic structure of SrTiO₃ is schematically shown in Figure 2. The valence band is primarily composed of oxygen p -states (T_{1u}) and the conduction band is composed of Ti- d states (T_{2g}). To estimate the effective magnetic field imposed on the electrons by axial phonons, we discuss the level splitting of Γ -point states transforming as $p_{\pm} = (p_x \pm ip_y)/\sqrt{2}$. Hence, we evaluate the overlap elements $\mathcal{H}_{\text{eff}}^{xy}(\mathbf{0})$ and $\mathcal{H}_{\text{eff}}^{yx}(\mathbf{0})$ in the effective Hamiltonian (12). Here, we use two assumptions. First, the electron-phonon coupling elements $g_{an\nu}$ are subject to selection rules [29, 30]. As both, the phonon mode and the p -orbitals are parity-odd, the overlap needs to involve parity-even orbitals, i.e., the Ti- d -states. Second the perturbative sum in (12) rapidly decreases with the spectral distance, $\mathcal{H}_{\text{eff}}^{ab} \sim E_{nb}^{-2}$ for $E_{nb} \gg \hbar\omega$. Using these assumptions and cubic symmetry, we derive (details given in the supplementary materials),

$$\mathcal{H}_{\text{eff}}^{xy}(\mathbf{0}) = -\mathcal{H}_{\text{eff}}^{yx}(\mathbf{0}), \quad (13)$$

$$\mathcal{H}_{\text{eff}}^{xy}(\mathbf{0}) = -\frac{i}{2}(\hat{a}_{\mathbf{0},\nu} + \hat{a}_{\mathbf{0},\nu}^\dagger)(\hat{a}_{\mathbf{0},\mu}^\dagger + \hat{a}_{\mathbf{0},\mu}) \frac{\hbar\omega |g|^2}{\Delta^2 - \hbar^2\omega^2}. \quad (14)$$

A basis transform to $p_{\pm} = (p_x \pm ip_y)/\sqrt{2}$, i.e., $H_{\text{eff}}^{\pm\pm} = \pm i\mathcal{H}_{\text{eff}}^{xy}$ gives a two-phonon amplitude

$$E^{\pm} = \pm \frac{1}{2} \frac{\hbar\omega |g|^2}{\Delta^2 - \hbar^2\omega^2}. \quad (15)$$

At room temperature, the infrared-active ferroelectric soft-mode in SrTiO₃ has a frequency of 2.7 THz [5, 31], i.e., $\hbar\omega \approx 11$ meV. In contrast, the measured direct band gap of SrTiO₃ is $\Delta \approx 3.75$ eV [32]. If we assume an electron phonon coupling of $g \approx 5$ meV [33], we obtain $\Delta E = E^+ - E^- \approx 4 \times 10^{-6}$ eV. If we compare this to the expected Zeeman splitting due to a magnetic field,

$$\frac{\Delta E}{2} = gJ\mu_B B_z^{\text{eff}}, \quad (16)$$

we obtain an effective magnetic field of $B^{\text{eff}} \approx 34$ mT for $J = 1$. This result is in very close agreement with

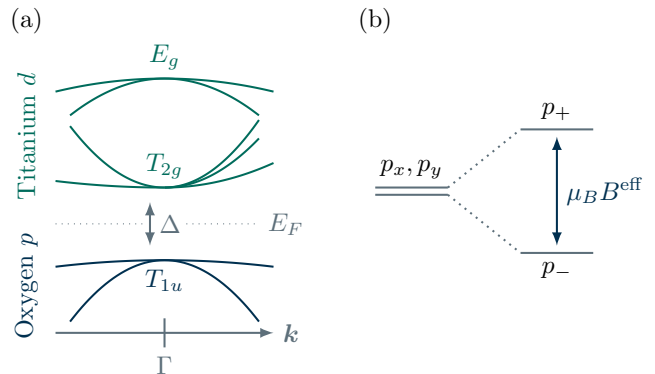


FIG. 2: Schematic of the electronic structure of SrTiO₃. (a) Orbital character of valence and conduction bands. (b) Splitting of p -orbitals in the effective magnetic field.

the experimental result of 32 mT reported by Basini *et al.* [5]. We stress that the effective magnetic field is not a "physical" magnetic field as described by Maxwell's equations. Still, it provides a time-reversal symmetry breaking field. Recently, Merlin [23] pointed out that by probing a material with the magneto-optical Kerr effect, such a time-reversal symmetry breaking field, or non-Maxwellian field, leads to a Kerr rotation of the linearly polarized probe laser, with electric field ϵ . This process can be described phenomenologically by the following free energy

$$F_{\text{MOKE}} = i\Lambda B^{\text{eff}}(\epsilon \times \epsilon^*), \quad (17)$$

where the Kerr rotation results from the difference of the dielectric constants for left- and right-circularly polarized light, in the presence of circularly polarized phonons and a resulting effective magnetic field,

$$\Delta\epsilon_R = -4\pi\Lambda B^{\text{eff}}, \quad \Delta\epsilon_L = 4\pi\Lambda B^{\text{eff}}. \quad (18)$$

Equation (18) follows a similar derivation as shown in equation (5) [25].

In the experiment reported by Basini *et al.* [5], circularly polarized phonons in SrTiO₃ were induced by a circularly polarized laser field. Due screening in the material, the penetration depth of the laser pump-pulse, measured by the decay length l_{decay} is in the order of $l_{\text{decay}} \approx 2.5 \mu\text{m}$. Hence, the expected Faraday rotation can be estimated as follows [5, 34],

$$\theta_F = \frac{l_{\text{decay}}V}{2} B_z^{\text{eff}} = \frac{l_{\text{decay}}V}{4} \frac{1}{\mu_B} \frac{\hbar\omega |g|^2}{\Delta^2 - \hbar^2\omega^2}. \quad (19)$$

Here, V is the Verdet constant of the material, which is $V \approx 180 \text{ rad m}^{-1} \text{ T}^{-1}$ for SrTiO₃ [5].

IV. DISCUSSION & SUMMARY

To highlight the fact that phonon inverse Faraday effect arises from circularly polarized phonons, we consider

the ladder operators $(\hat{a}_{\mathbf{0},\mu} + \hat{a}_{\mathbf{0},\mu}^\dagger)(\hat{a}_{\mathbf{0},\nu}^\dagger + \hat{a}_{\mathbf{0},\nu})$ in the effective Hamiltonian (14), and define $\hat{O}_\mu = \hat{a}_{\mathbf{0},\mu} + \hat{a}_{\mathbf{0},\mu}^\dagger$ and $\hat{O}_\nu = \hat{a}_{\mathbf{0},\nu} + \hat{a}_{\mathbf{0},\nu}^\dagger$, respectively. These operators describe the amplitude of the corresponding phonon modes μ and ν . Similarly to Ref. [19], we introduce operators $\hat{O}_\pm = (\hat{O}_\mu \pm i\hat{O}_\nu) / \sqrt{2}$, which allows us to write the effective Hamiltonian (14) as

$$\mathcal{H}_{\text{eff}}^{\pm\pm}(\mathbf{0}) = \mp \frac{i}{4} \left(\hat{O}_+ \hat{O}_+ - \hat{O}_- \hat{O}_- \right) \frac{\hbar\omega |g|^2}{\Delta^2 - \hbar^2\omega^2}. \quad (20)$$

Finally, we would like to relate our result to other theories on the problem. We note that equation (12) is a generalization of the orbit-lattice coupling described by Chaudhary *et al.* [19]. In the 4f paramagnets such as CeCl₃, the spectral distance E_{nb} is dominated by either spin-orbit interaction (≈ 0.1 eV) or by the crystal field splitting (6 meV). As a result, the expected effective magnetic field is significantly larger as compared to SrTiO₃. In fact, this is consistent with experimental work [6, 10] as well as theoretical estimates [19, 35]. The argument of tiny spectral gaps due to crystal field effects is also found in connection to a dynamical crystal field effect imposed by the phonon [22]. Furthermore, for materials with large gap $\Delta \gg \hbar\omega$, the denominator of the effective magnetic field becomes independent of the phonon frequency, i.e., $\Delta^2 - \hbar^2\omega^2 \approx \Delta^2$. In this limit, the level splitting is linearly dependent of the phonon frequency, $\Delta E \sim \hbar\omega$, which is related to the inertial effects discussed in Refs. [17, 18]. The same strong suppression of the expected effective magnetic field or magnetization by the band gap, $B^{\text{eff}} \sim \Delta^{-2}$, found in the present work, is also revealed in the formalism of the modern theory of

magnetization and the phonon magnetic moment from electronic topology [21, 36].

In summary, the approach presented here provides a general and material-independent framework for estimating an emergent magnetization and effective magnetic field due to axial phonons, i.e., phonons carrying angular momentum [15]. Furthermore, the result given by equation (12) highlights an important distinction between the phonon inverse Faraday effect and the optical inverse Faraday effect. While the microscopic theory of the optical inverse Faraday is based on the dipole coupling of the electric field to the electron, the phonon inverse Faraday effect is based on the electron-phonon interaction. As such the phonon inverse Faraday effect also occurs in the absence of a laser field, as long as an imbalance of left- and right-circularly polarized phonons is present. However, it is also worth noting that the circularly polarized phonons can be induced by a circularly polarized laser field [5]. Hence, for laser excitations resonant with phonons, both the phononic and the optical contribution coexist.

ACKNOWLEDGMENTS

We acknowledge inspiring discussions with Dominik Juraschek, Hanyu Zhu, Martina Basini, Stefano Bonetti, Alexander Balatsky, Finja Tietjen. Also, we acknowledge support from the Swedish Research Council (VR starting Grant No. 2022-03350), the Olle Engkvist Foundation, the Royal Physiographic Society in Lund and Chalmers University of Technology via the Department of Physics, and the areas of advance Nano and Materials.

In the process of finalizing this work, another interesting paper appeared discussing a similar approach [24].

-
- [1] Y. T. Rebane, Faraday effect produced in the residual ray region by the magnetic moment of an optical phonon in an ionic crystal, *Journal of Experimental and Theoretical Physics* **84**, 2323 (1983).
 - [2] D. M. Juraschek, M. Fechner, A. V. Balatsky, and N. A. Spaldin, Dynamical multiferroicity, *Physical Review Materials* **1**, 014401 (2017).
 - [3] D. M. Juraschek and N. A. Spaldin, Orbital magnetic moments of phonons, *Physical Review Materials* **3**, 064405 (2019).
 - [4] R. M. Geilhufe, V. Juričić, S. Bonetti, J.-X. Zhu, and A. V. Balatsky, Dynamically induced magnetism in KTaO₃, *Physical Review Research* **3**, L022011 (2021).
 - [5] M. Basini, M. Pancaldi, B. Wehinger, M. Udina, V. Unikandanunni, T. Tadano, M. C. Hoffmann, A. V. Balatsky, and S. Bonetti, Terahertz electric-field-driven dynamical multiferroicity in SrTiO₃, *Nature* 10.1038/s41586-024-07175-9 (2024).
 - [6] J. Luo, T. Lin, J. Zhang, X. Chen, E. R. Blackert, R. Xu, B. I. Yakobson, and H. Zhu, Large effective magnetic fields from chiral phonons in rare-earth halides, *Science* **382**, 698 (2023).
 - [7] B. Cheng, T. Schumann, Y. Wang, X. Zhang, D. Barbalas, S. Stemmer, and N. Armitage, A large effective phonon magnetic moment in a Dirac semimetal, *Nano letters* **20**, 5991 (2020).
 - [8] A. Baydin, F. G. Hernandez, M. Rodriguez-Vega, A. K. Okazaki, F. Tay, I. G. Timothy Noe, I. Katayama, J. Takeda, H. Nojiri, P. H. Rappl, *et al.*, Magnetic control of soft chiral phonons in PbTe, *Physical Review Letters* **128**, 075901 (2022).
 - [9] F. G. Hernandez, A. Baydin, S. Chaudhary, F. Tay, I. Katayama, J. Takeda, H. Nojiri, A. K. Okazaki, P. H. Rappl, E. Abramof, *et al.*, Chiral phonons with giant magnetic moments in a topological crystalline insulator, arXiv preprint arXiv:2208.12235 10.48550/arXiv.2208.12235 (2022).
 - [10] G. Schaack, Magnetic phonon splitting in rare earth trichlorides, *Physica B+C* **89**, 195 (1977).
 - [11] D. M. Juraschek, P. Narang, and N. A. Spaldin, Phonomagnetic analogs to opto-magnetic effects, *Physical Review Research* **2**, 043035 (2020).
 - [12] C. S. Davies, F. G. N. Fennema, A. Tsukamoto, I. Razdolski, A. V. Kimel, and A. Kirilyuk, Phononic switching

- of magnetization by the ultrafast Barnett effect, *Nature* **628**, 540 (2024).
- [13] S. J. Barnett, Magnetization by rotation, *Physical Review* **6**, 239 (1915).
- [14] A. Einstein, Experimenteller Nachweis der Ampèreschen Molekularströme, *Die Naturwissenschaften* **3**, 237 (1915).
- [15] L. Zhang and Q. Niu, Angular momentum of phonons and the Einstein–de Haas effect, *Physical Review Letters* **112**, 085503 (2014).
- [16] S. R. Tauchert, M. Volkov, D. Ehberger, D. Kazenwadel, M. Evers, H. Lange, A. Donges, A. Book, W. Kreuzpaintner, U. Nowak, and P. Baum, Polarized phonons carry angular momentum in ultrafast demagnetization, *Nature* **602**, 73 (2022).
- [17] R. M. Geilhufe, Dynamic electron-phonon and spin-phonon interactions due to inertia, *Physical Review Research* **4**, L012004 (2022).
- [18] R. M. Geilhufe and W. Hergert, Electron magnetic moment of transient chiral phonons in KTaO_3 , *Physical Review B* **107**, L020406 (2023).
- [19] S. Chaudhary, D. M. Juraschek, M. Rodriguez-Vega, and G. A. Fiete, Giant effective magnetic moments of chiral phonons from orbit-lattice coupling, arXiv preprint arXiv:2306.11630 10.48550/arXiv.2306.11630 (2023).
- [20] J. Fransson, Chiral phonon induced spin polarization, *Physical Review Research* **5**, L022039 (2023).
- [21] Y. Ren, C. Xiao, D. Saporov, and Q. Niu, Phonon magnetic moment from electronic topological magnetization, *Physical Review Letters* **127**, 186403 (2021).
- [22] L. Klebl, A. Schobert, G. Sangiovanni, A. V. Balatsky, and T. O. Wehling, Ultrafast pseudomagnetic fields from electron-nuclear quantum geometry, arxiv:2403.13070 10.48550/arXiv.2403.13070 (2024).
- [23] R. Merlin, Unraveling the effect of circularly polarized light on reciprocal media: Breaking time reversal symmetry with non-Maxwellian magnetic-esque fields, arxiv:2309.13622 10.48550/arXiv.2309.13622 (2023).
- [24] R. Merlin, Magnetophonics and the chiral phonon misnomer, arxiv:2404.19593 10.48550/arXiv.2404.19593 (2024).
- [25] P. Pershan, J. Van der Ziel, and L. Malmstrom, Theoretical discussion of the inverse Faraday effect, Raman scattering, and related phenomena, *Physical review* **143**, 574 (1966).
- [26] L. Liang, P. O. Sukhachov, and A. V. Balatsky, Axial magnetoelectric effect in Dirac semimetals, *Physical Review Letters* **126**, 247202 (2021).
- [27] J.-J. Zhou, O. Hellman, and M. Bernardi, Electron-phonon scattering in the presence of soft modes and electron mobility in SrTiO_3 perovskite from first principles, *Physical Review Letters* **121**, 226603 (2018).
- [28] F. Giustino, Electron-phonon interactions from first principles, *Reviews of Modern Physics* **89**, 015003 (2017).
- [29] L. Shu, Y. Xia, B. Li, L. Peng, H. Shao, Z. Wang, Y. Cen, H. Zhu, and H. Zhang, Full-landscape selection rules of electrons and phonons and temperature-induced effects in 2d silicon and germanium allotropes, *npj Computational Materials* **10**, 2 (2024).
- [30] Y. Chen, Y. Wu, B. Hou, J. Cao, H. Shao, Y. Zhang, H. Mei, C. Ma, Z. Fang, H. Zhu, and H. Zhang, Renormalized thermoelectric figure of merit in a band-convergent $\text{Sb}_2\text{Te}_2\text{Se}$ monolayer: full electron–phonon interactions and selection rules, *Journal of Materials Chemistry A* **9**, 16108 (2021).
- [31] H. Vogt, Refined treatment of the model of linearly coupled anharmonic oscillators and its application to the temperature dependence of the zone-center soft-mode frequencies of KTaO_3 and SrTiO_3 , *Physical Review B* **51**, 8046 (1995).
- [32] K. van Benthem, C. Elsässer, and R. H. French, Bulk electronic structure of SrTiO_3 : Experiment and theory, *Journal of Applied Physics* **90**, 6156 (2001).
- [33] J.-J. Zhou, O. Hellman, and M. Bernardi, Electron-phonon scattering in the presence of soft modes and electron mobility in SrTiO_3 perovskite from first principles, *Physical Review Letters* **121**, 226603 (2018).
- [34] M. Freiser, A survey of magneto-optic effects, *IEEE Transactions on Magnetics* **4**, 152 (1968).
- [35] D. M. Juraschek, T. c. v. Neuman, and P. Narang, Giant effective magnetic fields from optically driven chiral phonons in 4f paramagnets, *Physical Review Research* **4**, 013129 (2022).
- [36] D. Saporov, B. Xiong, Y. Ren, and Q. Niu, Lattice dynamics with molecular berry curvature: Chiral optical phonons, *Physical Review B* **105**, 064303 (2022).
- [37] W. Hergert and R. M. Geilhufe, *Group Theory in Solid State Physics and Photonics: Problem Solving with Mathematica* (Wiley-VCH, 2018) ISBN: 978-3-527-41133-7.
- [38] R. M. Geilhufe and W. Hergert, GTPack: A Mathematica Group Theory Package for Application in Solid-State Physics and Photonics, *Frontiers in Physics* **6**, 86 (2018).

Supplementary Materials: Phonon Inverse Faraday effect from electron-phonon coupling

Natalia Shabala and R. Matthias Geilhufe

Department of Physics, Chalmers University of Technology, 412 96 Göteborg, Sweden

SINGLE ION

The perturbation due to lattice vibrations has the form

$$V(t) = 2\Re[\mathbf{u} \cdot \nabla_{\mathbf{u}} U]. \quad (21)$$

It can be written as harmonic perturbation $V(t) = ve^{i\omega t} + v^*e^{-i\omega t}$, with perturbation amplitude v given by

$$v = \mathbf{u} \cdot \nabla U. \quad (22)$$

We define two potential operators U_{\pm} , as $U_{\pm} = \left(\frac{\partial U}{\partial u_x} \pm i\frac{\partial U}{\partial u_y}\right)/\sqrt{2}$. Thus the perturbation amplitude can be expressed as

$$v = u_R \nabla U_+ + u_L \nabla U_-. \quad (23)$$

Now we can derive the expression for the effective Hamiltonian starting with the equation derived by Pershan et al. [25]

$$\langle a | H_{\text{eff}}(t) | b \rangle = - \sum_n \left[\frac{\langle a | v | n \rangle \langle n | v^* | b \rangle}{E_{nb} - \hbar\omega} - \frac{\langle a | v^* | n \rangle \langle n | v | b \rangle}{E_{nb} + \hbar\omega} \right]. \quad (24)$$

The form of the perturbation amplitude in equation (23) combined with the effective Hamiltonian (24), gives us

$$\begin{aligned} \mathcal{H}_{\text{eff}}^{ab} = & - \sum_n \left[\frac{E_{nb}}{E_{nb}^2 - \hbar^2\omega^2} \left((u_R u_R^* + u_L u_L^*) (\nabla U_+^{an} \nabla U_-^{an} + \nabla U_-^{an} \nabla U_+^{an}) + \right. \right. \\ & \left. \left. + 2u_L u_R^* \nabla U_-^{an} \nabla U_-^{an} + 2u_L^* u_R \nabla U_+^{an} \nabla U_+^{an} \right) + \right. \\ & \left. + \frac{\hbar\omega}{E_{nb}^2 - \hbar^2\omega^2} (u_R u_R^* - u_L u_L^*) (\nabla U_+^{an} \nabla U_-^{an} - \nabla U_-^{an} \nabla U_+^{an}) \right]. \end{aligned} \quad (25)$$

Here, only $(u_R u_R^* - u_L u_L^*)$ transforms as a magnetic field therefore this term is the only relevant term and all others can be discarded. In Cartesian coordinates this gives us

$$\mathcal{H}_{\text{eff}}^{ab} = -(\mathbf{u} \times \mathbf{u}^*)_z \sum_n \frac{\hbar\omega}{E_{nb}^2 - \hbar^2\omega^2} (\nabla U_+^{an} \times \nabla U_-^{an})_z. \quad (26)$$

ENTIRE CRYSTAL

To derive the expression for the effective Hamiltonian for the entire crystal, we introduce phonon displacement amplitudes $u_{p\mu}$ and $u_{p'\nu}$ for phonon modes μ, ν and unit cells p and p' . Then we can use these phonon modes to define the effective Hamiltonian by analogy with (9):

$$\mathcal{H}_{\text{eff}}^{ab} = -\frac{\hbar\omega}{4} \sum_{n,p,p'} (u_{p\mu} u_{p'\nu}^* - u_{p'\nu} u_{p\mu}^*) \frac{\langle a | \frac{\partial U}{\partial u_{p\mu}} | n \rangle \langle n | \frac{\partial U}{\partial u_{p'\nu}} | b \rangle - \langle a | \frac{\partial U}{\partial u_{p'\nu}} | n \rangle \langle n | \frac{\partial U}{\partial u_{p\mu}} | b \rangle}{E_{nb}^2 - \hbar^2\omega^2}. \quad (27)$$

Given (1), for circularly polarized phonons we quantize the phonon displacement in the following way

$$\begin{aligned} u_{p\mu} &= i \sum_{\mathbf{q}} e^{i\mathbf{q} \cdot \mathbf{R}_p} l_{\mathbf{q}\mu} (\hat{a}_{\mathbf{q}\mu} + \hat{a}_{-\mathbf{q}\mu}^\dagger) \\ u_{p\nu} &= \sum_{\mathbf{q}} e^{i\mathbf{q} \cdot \mathbf{R}_p} l_{\mathbf{q}\nu} (\hat{a}_{\mathbf{q}\nu} + \hat{a}_{-\mathbf{q}\nu}^\dagger) \end{aligned} \quad (28)$$

where $l_{\mathbf{q}\nu} = \sqrt{\frac{\hbar}{2M_0\omega_{\mathbf{q}\nu}}}$ denotes the zero displacement amplitude with M_0 being a reference mass. Operators $\hat{a}_{\mathbf{q}\nu}^\dagger$ and $\hat{a}_{\mathbf{q}\nu}$ are bosonic creation and annihilation operators and operator $(\hat{a}_{\mathbf{q}\nu} + \hat{a}_{-\mathbf{q}\nu}^\dagger)$ can be interpreted as phonon displacement operator.

Here it is useful to introduce electron-phonon matrix elements $g_{mn\nu}(\mathbf{k}, \mathbf{q})$ [28]:

$$g_{mn\nu}(\mathbf{k}, \mathbf{q}) = \langle m, \mathbf{k} + \mathbf{q} | \sum_p l_{\mathbf{q}\nu} e^{i\mathbf{q}\cdot\mathbf{R}_p} \frac{\partial U}{\partial u_{p\nu}} | n, \mathbf{k} \rangle. \quad (29)$$

With equation (10) and equation (11) we can express the effective Hamiltonian (27) in terms of electron-phonon matrix elements $g_{an\nu}(\mathbf{k}, \mathbf{q})$, $g_{bn\mu}(\mathbf{k}, \mathbf{q}')$ and quantized displacement operators $(\hat{a}_{\mathbf{q}\mu} + \hat{a}_{-\mathbf{q}\mu}^\dagger)$, $(\hat{a}_{\mathbf{q}'\nu} + \hat{a}_{-\mathbf{q}'\nu}^\dagger)$. We consider an effective Hamiltonian that is diagonal in wave vector \mathbf{k} . Therefore in $\langle a, \mathbf{k} | e^{i\mathbf{q}\cdot\mathbf{R}_p} \frac{\partial U}{\partial u_{p\mu}} | n, \mathbf{k}' \rangle \langle n, \mathbf{k}' | e^{-i\mathbf{q}'\cdot\mathbf{R}_{p'}} \frac{\partial U}{\partial u_{p'\nu}} | b, \mathbf{k} \rangle$ it must be true that $\mathbf{k} = \mathbf{k}' + \mathbf{q}$ and $\mathbf{k}' - \mathbf{q}'$. Thus $\mathbf{q} = \mathbf{q}'$. Thus the effective Hamiltonian is given by

$$\mathcal{H}_{\text{eff}}^{ab}(\mathbf{k}) = -i \frac{\hbar\omega}{2} \sum_{\mathbf{q}} \left[(\hat{a}_{\mathbf{q},\mu} + \hat{a}_{-\mathbf{q},\mu}^\dagger)(\hat{a}_{-\mathbf{q},\nu}^\dagger + \hat{a}_{\mathbf{q},\nu}) \times \sum_n \frac{g_{an\mu}(\mathbf{k}, \mathbf{q})g_{bn\nu}^*(\mathbf{k}, \mathbf{q}) - g_{an\nu}(\mathbf{k}, \mathbf{q})g_{bn\mu}^*(\mathbf{k}, \mathbf{q})}{E_{\mathbf{k}nb}^2 - \hbar^2\omega^2} \right]. \quad (30)$$

EFFECTIVE MAGNETIC FIELD

We consider cubic symmetry and the interaction of electronic states with a Γ -point infrared-active phonon, transforming as the irreducible representation T_{1u} . The electron-phonon coupling elements are subject to selection rules[29, 30], where electrons from an orbital transforming as D^n are allowed to scatter to an orbital transforming as D^a iff D^a occurs on the right-hand side of the Clebsch-Gordan decomposition,

$$T_{1u} \otimes D^n \simeq N_1 D^1 \oplus N_2 D^2 \oplus \dots \quad (31)$$

N_a is the number of times D^a occurs within the Clebsch-Gordan sum (31). The electron-phonon matrix element relates to the Wigner-Eckart theorem [37],

$$g_{an\nu} = g_{D^a\alpha; D^n\eta; T_{1u}\nu} = \sum_{\xi=1}^{N_a} \left(\begin{matrix} D^n & T_{1u} \\ \eta & \nu \end{matrix} \middle| \begin{matrix} D^a \\ \alpha, \xi \end{matrix} \right)^* (D^a | T_{1u} | D^n), \quad (32)$$

with the sum running over a product of Clebsch-Gordan coefficients and reduced matrix elements. We estimate the effective magnetic field in SrTiO₃ by assuming oxygen p -states. The p states at the Γ -point ($\mathbf{k} = 0$) transform as the irreducible representation T_{1u} . We decompose the direct product of the irreducible representations of the p -orbitals (T_{1u}) and the infrared active phonon mode (T_{1u}),

$$T_{1u} \otimes T_{1u} \sim A_{1g} \oplus T_{1g} \oplus T_{2g} \oplus E_g. \quad (33)$$

Hence, the overlap is only non-zero if the p -electron scatters into an s or d state, with representations A_{1g} or E_g and T_{2g} , respectively. Furthermore, we notice that $N_n = 1$ in either case. According to equation (12), the perturbative series is suppressed by the size of the spectral distance squared, $1/\omega_{nb}^2$, $\omega \ll \omega_{nb}$ and it suffices to only consider the overlap between T_{1u} and T_{2g} states, corresponding to the band gap $\Delta \approx 3.25$ eV [32]. Hence, the overlap element for p_x and p_y in the effective Hamiltonian (12), for electrons at $\mathbf{k} = 0$ and phonons at $\mathbf{q} = 0$, is given by

$$\mathcal{H}_{\text{eff}}^{xy}(\mathbf{k} = 0) = -i(\hat{a}_{\mathbf{0},\nu} + \hat{a}_{\mathbf{0},\nu}^\dagger)(\hat{a}_{\mathbf{0},\mu}^\dagger + \hat{a}_{\mathbf{0},\mu}) \frac{\hbar\omega |g|^2}{\Delta^2 - \hbar^2\omega^2} \sum_{\eta} \left[\left(\begin{matrix} T_{2g} & T_{1u} \\ \eta & \nu \end{matrix} \middle| \begin{matrix} T_{1u} \\ x \end{matrix} \right)^* \left(\begin{matrix} T_{2g} & T_{1u} \\ \eta & \mu \end{matrix} \middle| \begin{matrix} T_{1u} \\ y \end{matrix} \right) - \left(\begin{matrix} T_{2g} & T_{1u} \\ \eta & \mu \end{matrix} \middle| \begin{matrix} T_{1u} \\ x \end{matrix} \right)^* \left(\begin{matrix} T_{2g} & T_{1u} \\ \eta & \nu \end{matrix} \middle| \begin{matrix} T_{1u} \\ y \end{matrix} \right) \right]. \quad (34)$$

electron	T_{1u}	p_x				p_y				p_z
phonon	T_{1u}	x	y	z	x	y	z	x	y	z
T_{2g}	xz	0	0	$\frac{1}{\sqrt{2}}$	0	0	0	$\frac{1}{\sqrt{2}}$	0	0
	yz	0	0	0	0	0	$\frac{1}{\sqrt{2}}$	0	$\frac{1}{\sqrt{2}}$	0
	xy	0	$\frac{1}{\sqrt{2}}$	0	$\frac{1}{\sqrt{2}}$	0	0	0	0	0

TABLE I: Relevant Clebsch-Gordan coefficients

Here we introduced g as the reduced matrix element. Equation (34) can be evaluated from the Clebsch-Gordan coefficients calculated using GTPack [37, 38] and given in Table I,

$$\mathcal{H}_{\text{eff}}^{xy}(\mathbf{k} = 0) = -\mathcal{H}_{\text{eff}}^{yx}(\mathbf{k} = 0) = -\frac{i}{2}(\hat{a}_{\mathbf{0},\nu} + \hat{a}_{\mathbf{0},\nu}^\dagger)(\hat{a}_{\mathbf{0},\mu}^\dagger + \hat{a}_{\mathbf{0},\mu}) \frac{\hbar\omega |g|^2}{\Delta^2 - \hbar^2\omega^2}. \quad (35)$$